

CNOS: A Strong Baseline for CAD-based Novel Object Segmentation

Van Nguyen Nguyen¹, Tomas Hodan², Georgy Ponimatkin¹, Thibault Groueix³, Vincent Lepetit¹

¹LIGM, Ecole des Ponts, ²Reality Labs at Meta, ³Adobe

Abstract

We propose a simple three-stage approach to segment unseen objects in RGB images using their CAD models. Leveraging recent powerful foundation models, DINOv2 and Segment Anything, we create descriptors and generate proposals, including binary masks for a given input RGB image. By matching proposals with reference descriptors created from CAD models, we achieve precise object ID assignment along with modal masks. We experimentally demonstrate that our method achieves state-of-the-art results in CAD-based novel object segmentation, surpassing existing approaches on the seven core datasets of the BOP challenge by 19.8% AP using the same BOP evaluation protocol. Our source code is available at <https://github.com/nv-nguyen/cnos>.

1. Introduction

Pose estimation plays a critical role in various applications of robotics and augmented reality. While existing deep learning methods have achieved remarkable performance for seen objects, they heavily rely on extensive training data specific to each target object [15, 22, 23]. However, introducing previously-unseen objects necessitates significant time and effort to synthesize or annotate data and retrain the model. This limitation restricts the practical application of pose estimation in the industry despite its huge potential. For instance, in a logistic warehouse, it appears impractical to retrain the pose estimation method for every new product reference.

Performing objects pose estimation commonly involve two main steps. Firstly, an instance segmentation or object detection method is employed to locate or segment objects in 2D images. The results of this step are then used in the subsequent pose estimation step to accurately estimate 6D object pose. Recent works such as template-pose [18] and MegaPose [16] have introduced effective CAD-based object pose estimation methods. However, these methods mainly focus on the second step of pose estimation pipeline and overlook the crucial initial step of object detection or segmentation. They require input 2D bounding boxes, which

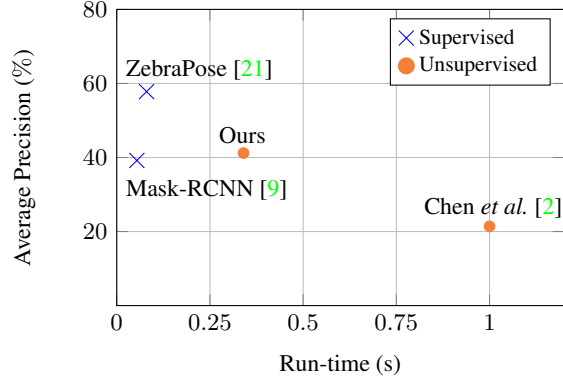


Figure 1. **Performance on seven core datasets of BOP challenge [22].** Our method relies on SAM [14, 27] for segmentation and on DINOv2 [19] for visual features. We also incorporate photo-realistic rendering techniques that compute the Global Illumination in the 3D scene by simulation light bounces - BlenderProc [3]. We significantly improves over Chen *et al.* [2]. Additionally, we outperform the supervised method Mask-RCNN [9] which was used in CosyPose [15].

restricts their applicability to scenarios where precise 2D bounding box is readily available.

We aim to overcome both of these limitations *i.e.* propose a method that tackle the first part of the pose estimation pipeline, detecting and segmenting objects in images from their CAD model only, and that generalize to images of novel object. Recent work [2] revealed a significant performance gap on novel objects compared to objects available for training such a model. We present a simple approach, which we call **CNOS** for **CAD-based Novel Object Segmentation**. As illustrated in Figure 1, CNOS relies on DINOv2 [19] and leverages photo-realistic rendering techniques (BlenderProc [3]). It significantly improves the accuracy of novel segmentation compared to Chen *et al.* [2] and outperforms the supervised method Mask-RCNN [9] which was used in CosyPose [15].

More precisely, CNOS consists of three stages: (i) in the onboarding stage, we create reference descriptors from CAD models using rendering synthetic images and DINOv2; (ii) in the proposal stage, given an RGB image, we generate object proposals using Segmenting Anything

(SAM) [14] or Fast Segmenting Anything (FastSAM) [27]; and (iii) in the matching stage, we compare descriptors to assign object ID for each proposal, enabling accurate object detection and segmentation. Extensive experiments on the seven core datasets of the BOP challenge [22] with the standard evaluation¹ validate the state-of-the-art performance of our method.

In summary, our contributions are:

- A simple yet powerful approach for CAD-based novel object segmentation, which significantly improve the state-of-the-art and outperforms the supervised Mask-RCNN [9] trained in CosyPose [15] on seven core datasets of the BOP challenge;
- Extensive comparisons between foundation models for image segmentation, including FastSAM [27] versus SAM [14], aimed at evaluating their performance in run-time efficiency;
- An ablation study on the onboarding stage by varying the number of viewpoints and the rendering engine with CAD models.

2. Related work

In this section, we provide a brief overview of existing works on object segmentation commonly used in 6D object pose estimation.

Seen object segmentation. Most of the existing object pose estimation methods [15, 23] employ object segmentation such as Mask-RCNN [9] as the initial stage, typically retrained on extensive training data specific to each target object [22]. This data-driven approach aims to enhance the robustness in challenging scenarios with heavy occlusions or extreme lighting variations. However, these methods often neglect the detection or segmentation of novel objects, which is often more practical. In this work, we address this limitation by focusing on the segmentation of previously-unseen objects from their CAD models without retraining.

Unseen object segmentation. Object segmentation methods have traditionally focused on scenarios known as “closed-world” settings, where the training and test sets share the same object classes. Nevertheless, recent observations by Du *et al.* [6, 7] suggest that class-agnostic instance segmentation networks can effectively generalize to previously unseen object classes, which holds potential for advancing segmentation-based 6D pose estimation or tracking. In line with this, Nguyen *et al.* [17] have proposed a two-stage 6D tracking approach based on these observations. Their approach assumes the availability of an initial bounding box to segment objects using [6] then propagate

it to next frames using optical flow. Subsequently, 6D novel object tracking is performed based on the predicted object masks. In contrast, our objective solely focuses on segmenting objects in images derived from CAD models without initial boxes, aiming to facilitate the development of scalable CAD-based pose estimation methods.

Commonly used in robotics, UOIS-Net [26] employs a two-stage approach to segment novel objects. Firstly, it operates solely on the depth channel to generate object instance center votes and assembles them into rough initial masks. These masks are subsequently refined using the RGB channel. Xiang *et al.* [25] also proposes a RGB-D based method that utilizes learned feature embeddings and applies a mean shift clustering algorithm to discover and segment unseen objects. It is worth noting that both UOIS-Net [26] and Xiang *et al.* [25] are RGB-D approaches, while our method targets the segmentation of unseen objects from only RGB images which is more challenging but more applicable.

Recently, Segment Anything (SAM) [14] has introduced a powerful foundation model for image segmentation capable of segmenting all objects in a given RGB image. Chen *et al.* [2] utilize SAM to extract object proposals, which are then combined with visual clues extracted by ImageBind [8]. Feature matching is subsequently applied for CAD-based novel object segmentation. We experimentally demonstrate the superiority of our method by using realistic rendering techniques BlenderProc [3] and DINOv2 [19] compared to [2]. Additionally, we conduct extensive experiments that highlight the benefits of employing FastSAM [27] to improve runtime efficiency and provide comprehensive study for CAD-based novel object segmentation.

3. Method

In this section, we provide a detailed description of our three-stage approach for CAD-based novel object segmentation. We first describe the onboarding stage in Section 3.1, where we extract visual descriptors from CAD models. In Section 3.2, we explain the proposal stage, which involves obtaining all possible masks and their descriptors. Finally, in Section 3.3, we discuss the matching stage, where object masks are retrieved and labeled based on visual descriptors of their CAD models.

3.1. Onboarding stage

In the onboarding stage, our objective is to leverage the 3D model clues for effective object segmentation. To achieve this, we employ offline rendering to generate a set of RGB synthetic templates then extract their visual descriptors using DINOv2 [19].

To ensure robust object segmentation under different orientations, we render CAD models under 42 viewpoints as shown in Figure 3. These 42 viewpoints are defined by

¹<https://bop.felk.cvut.cz/challenges/bop-challenge-2022/>

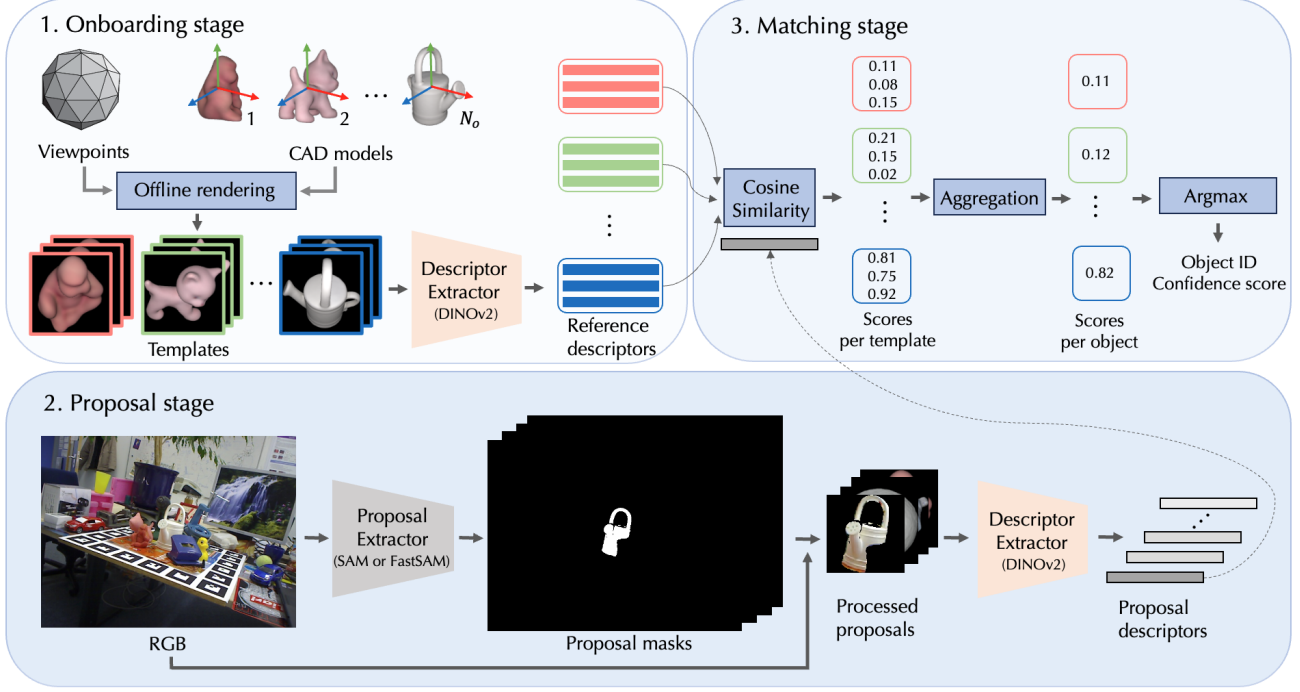


Figure 2. **Method overview.** Given a set of CAD models and a RGB image at run-time, our method first renders a set of templates and extracts their visual descriptors (Section 3.1). Then, we use a proposal network to segment all possible objects in 2D images and extracts their visual descriptors using the same descriptor network (Section 3.2). Finally, we match these two sets of descriptors using cosine similarity and apply view aggregation and argmax to assign an object ID to each proposal (Section 3.3).

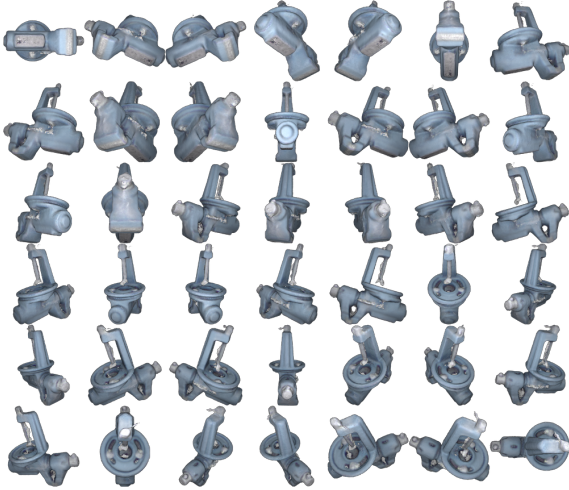


Figure 3. **Visualization of templates for the “benchwise” object in the Linemod dataset [10] rendered with Pyrender [20].** We show 42 templates rendered from viewpoints defined by a regular icosahedron, as depicted in [18], for effective template matching.

a regular icosahedron which has been shown in [18] to provide well-distributed coverage of CAD models in a 3D sphere for robust template matching. Additionally, we experiment with denser viewpoints by dividing each triangle of the icosahedron into four smaller triangles. This render-

ing process results in a total of $N_o \times V$ templates, where N_o is the number of testing CAD models, and V is the number of viewpoints.

We then crop the templates with the ground-truth bounding boxes and extract their visual descriptors as the “class-token” features of DINOv2 to generate a set of reference descriptors D_r of size $N_o \times V \times C$. By default, we use $V = 42$ and $C = 1024$.

3.2. Proposal stage

For each testing RGB image, we use SAM [14] or FastSAM [27] with a default configuration to generate a set of N_p unlabeled proposals, where each proposal i is characterized by a model mask M_i . It is worthy to note that N_p is not fixed and varies depending on the content of each testing RGB image.

To compute the visual descriptor for each proposal i , we first remove the background of the input RGB image using the corresponding mask M_i . Subsequently, we crop the image using the model bounding box derived from M_i . Since each proposal mask M_i has different bounding box sizes, parallel processing becomes unfeasible. To overcome this, we add a simple image processing step including scaling and padding in order to resize all proposals to a consistent size of 224×224 . This standardization enables efficient

parallel processing of proposals in a single batch.

Then, we extract visual descriptors from processed proposals using the “class-token” of DINOv2 [19] to generate a set of proposal descriptors \mathbf{D}_p of size $N_p \times C$.

3.3. Matching stage

The goal of the matching stage is to assign each proposal i a label object ID o_i and a confidence score s_i . To achieve this, we compare each proposal descriptor in \mathbf{D}_p with each template descriptor in \mathbf{D}_t by using the cosine similarity. This comparison step produces a similarity matrix of size $N_p \times N_o \times V$.

Views aggregation. By aggregating the similarity scores over all V templates for each CAD model, we obtain a matrix of size $N_p \times N_o$. This matrix represents the similarity between each proposal p_i and each CAD model. We experiment with different aggregation functions, such as Mean, Max, Median, and Mean of top k highest, noted Mean_k . Among these, we find that Mean_k yields the most robust results.

Object ID assignment. To assign the object ID o_i and confidence score s_i to each proposal, we simply apply the argmax and max function on the similarity matrix over the N_o objects.

At the end of this matching stage, we obtain a set of labeled proposals, where each proposal is defined as $\{M_i, o_i, s_i\}$ where M_i is the modal mask, o_i is the object ID, s_i is the confidence score.

4. Experiment

In this section, we first describe the experimental setup (Section 4.1). Then, we compare our method with previous works [2, 9, 21] on the seven core datasets of the BOP challenge [22] (Section 4.2). We conduct an ablation study to evaluate accuracy under different aggregating functions, different number of rendering viewpoints and provide its run-time (Section 4.3). Finally, we discuss its use in the 6D novel pose estimation pipeline (Section 4.4).

4.1. Experimental setup

Datasets. We evaluate our method on the test set of seven core datasets of the BOP challenge [22]: LineMod Occlusion (LMO) [1], T-LESS [11], TUD-L [12], IC-BIN [4], ITODD [5], HomebrewedDB (HB) [13] and YCB-Video (YCB-V) [24]. These datasets exhibit 132 different objects in total in cluttered scenes with occlusions. These datasets present many factors of variation: textured or untextured, symmetric or asymmetric, household or industrial.

Evaluation metric. We evaluate our method using the Average Precision (AP) metrics, following the COCO metric and the BOP Challenge evaluation protocol [22]. The AP metric is calculated as the mean of AP values at different Intersection over Union (IoU) thresholds ranging from 0.50 to 0.95 with an increment of 0.05.

Baselines. We compare our method with Chen *et al.* [2], the most relevant work to ours. They use a three-stage CAD-based object segmentation approach, incorporating SAM [14] for image segmentation and ImageBlind [8] for visual descriptor extraction. Their use of 72 templates per CAD model resulted in the best performance according to their paper. Additionally, we compare our method with two relevant supervised methods from the BOP challenge [22]: Mask RCNN [9], trained on real or synthetic training datasets specific to each test object used in CosyPose [15], and ZebraPose [21], which is currently the state-of-the-art for this task in the BOP challenge.

Implementation details. We use the default ViT-H SAM [14], as well as the default FastSAM [27], which has demonstrated promising results in terms of runtime efficiency, as the foundation models for the proposal stage. For extracting visual descriptors, we use the default ViT-H model of DINOv2 [19].

To further evaluate the performance of our method, we conducted a comparison using two sets of templates. The first set of templates was generated using Pyrender [20] from 42 pre-defined viewpoints. It is worthy to note that Pyrender compute the Direct Illumination and it is extremely fast, takes in average 0.026 second per image. The second set of templates comprised 42 physic-based rendering templates selected from the available synthetic images of the PBR-BlenderProc4BOP training set provided in the BOP challenge. These realistic templates were specifically chosen to closely match the orientations of the 42 pre-defined viewpoints in the first set.

In order to maintain a consistent runtime across all datasets, we resize the images while preserving their aspect ratio. Specifically, we ensure that the width of each input RGB testing image is fixed at 640 pixels. All our experiments were conducted on a single V100 GPU.

4.2. Comparison with the State-of-the-Art

In Table 1, we demonstrate that our proposed approach outperforms Chen *et al.* [2] by a significant margin of 19.8% in terms of AP metrics. Furthermore, despite not being trained on the testing objects of the BOP datasets, our method surpasses the performance of MaskRCNN [9] used in CosyPose [15], which was specifically trained on these objects. This highlights the effectiveness of our method,

	Method	Rendering	BOP Datasets						
			LM-O	T-LESS	TUD-L	IC-BIN	ITODD	HB	YCB-V
Supervised	1 MaskRCNN [9] (Synth) -	-	37.5	51.7	30.6	31.6	12.2	47.1	42.9
	2 MaskRCNN [9] (Real) -	-	37.5	54.4	48.9	31.6	12.2	47.1	42.9
	3 ZebraPose [21] (Synth) -	-	50.6	62.9	51.4	37.9	36.1	64.6	62.2
	4 ZebraPose [21] (Real) -	-	50.6	70.9	70.7	37.9	36.1	64.6	74.0
Unsupervised	5 Chen <i>et al.</i> [2]	-	17.6	9.6	24.1	18.7	6.3	31.4	41.9
	6 CNOS (SAM)	Pyrender [20]	33.3	38.3	35.8	27.2	14.8	45.9	57.6
	7 CNOS (SAM)	BlenderProc [3]	39.6	39.7	39.1	28.4	28.2	48.0	59.5
	8 CNOS (FastSAM)	BlenderProc [3]	39.7	37.4	48.0	27.0	25.4	51.1	59.9

Table 1. **Comparison of our method with [2, 9, 21] on the seven core datasets of the BOP challenge [22].** MaskRCNN and ZebraPose are retrained specifically on these objects with synthetic renderings of the CAD model (noted as “Synth”) or real images of the object (noted as “Real”). We classify them as “supervised” in contrast with [2] and our method which we call “unsupervised” because it requires no retraining for novel objects. We report the AP metric (higher is better) using the protocol from [22]. We highlight in **blue** the best supervised method and in **yellow** the best unsupervised method. Our method not only significantly outperforms [2] under the same settings but also surpasses the supervised method MaskRCNN, highlighting its ability to generalize.

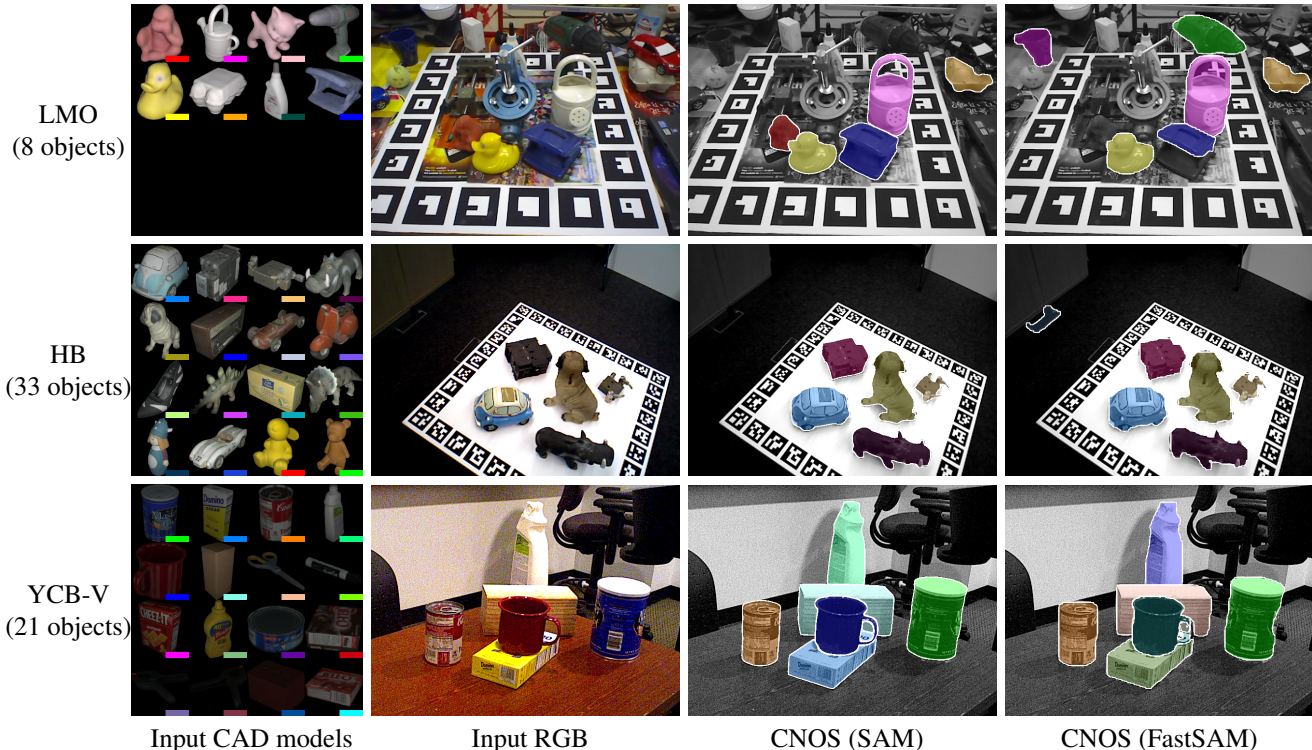


Figure 4. **Qualitative results on LMO [1], HB [13] and YCB-V [24].** The first image displays the input CAD models. In cases where there are more than 16 models, we only show the first 16 to ensure better visibility. The second image shows the input RGB image. The last two images depict the detections made by CNOS (SAM) and CNOS (FastSAM) with confidence scores greater than 0.5, ensuring improved visibility. Interestingly, although both CNOS (SAM) and CNOS (FastSAM) utilize DINOv2 [19] for visual descriptor extraction, their final predictions exhibit slight differences due to variations in their proposal sets.

leveraging the large-scale self-supervised model DINOv2 [19] and realistic rendering techniques BlenderProc [3].

Since the ground-truth masks of the BOP datasets are not all accessible, we could not quantitatively evaluate the different component of our pipeline independently on one an-

other, *i.e.* the errors made by our proposal networks (SAM, FastSAM) or our descriptor network (DINOv2). However, we qualitatively found that the proposal network makes very few mistakes and outputs a lot of proposals. Therefore, we hypothesize that DINOv2 is the current perfor-

Method	Viewpoint density	
	Coarse (42)	Dense (162)
CNOS (SAM)	39.6	39.5
CNOS (FastSAM)	39.7	39.7

Table 2. **Ablation study on the number of viewpoints on LMO dataset [1].** The denser viewpoints are created by subdividing each triangle of the icosahedron (used to create coarse viewpoints) into four smaller triangles.

Method	Aggregating function			
	Mean	Median	Max	Mean _k
CNOS (SAM)	36.6	34.9	39.1	39.6
CNOS (FastSAM)	36.2	33.8	39.7	39.7
Average	36.40	34.40	39.40	39.65

Table 3. **Ablation study on aggregating functions on the LMO dataset [1].** Using the Mean_k function, which calculates the average of the top k (k=5) highest values, yields the best performance for our method.

mance bottleneck, and it is where improvements can still be made in the pipeline to close the gap with supervised state-of-the-art approaches like ZebraPose.

We show in Figure 4 qualitative results of our method on LMO [1], HB [13] and YCB-V [24] datasets.

4.3. Ablation study

Rendering. Table 1 demonstrates the performance of our method using two types of rendering: Pyrender [20] in row 6 and BlenderProc [3] in row 7. The results indicate that incorporating realistic rendering significantly bridges the gap between synthetic rendering and real testing images, improving 4.3% in AP metrics.

Number of viewpoints. As shown in Table 2, using more viewpoints does not bring any improvement compared to the coarse viewpoints. This can be explained by the fact that the current set of 42 coarse viewpoints already provides sufficient coverage of the 3D objects.

Aggregating function. We present the results of the ablation study in Table 3, which explores different types of aggregating functions for combining the similarity between reference descriptors created from rendering different viewpoints of CAD models and visual descriptors of proposals. Among the tested functions, Mean_k (k=5), which is the average of the k highest similarity, achieves the best performance.

Method	Run-time (second)		
	Onboarding	Proposal	Matching
CNOS (SAM, Pyrender)	1.22	1.58	0.13
CNOS (FastSAM, Pyrender)	1.22	0.22	0.12
CNOS (FastSAM, PBR)	42.1	0.22	0.12

Table 4. **Run-time.** We report the runtime of each stage of our method on a single V100 GPU. The runtime of the onboarding stage includes both the rendering time and the visual descriptor extraction time for each CAD model.

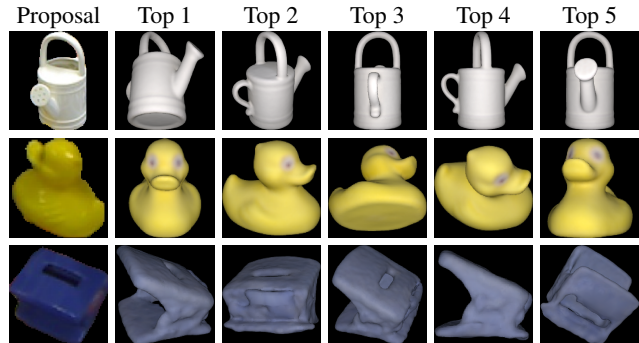


Figure 5. **Visualization of nearest neighbors.** We display the proposal in the first column along with the rendering of its five nearest neighbors given predicted object ID in the following five columns. While DINOv2’s features performs well on CAD-based novel object segmentation task, its does not perform well for pose estimation.

Run-time. In Table 4, we present the runtime of each stage in our method. In the onboarding stage, the average rendering time for one image with Pyrender [20] is 0.026 second while with BlenderProc [3] is around 1 second per image on a single V100 GPU. It is important to note that the onboarding stage is performed once for each CAD model. In terms of run-time, the onboarding stage is clearly bottlenecked by the generation of templates, while the proposal stage is currently bottlenecked by the segmentation algorithm.

4.4. Discussion

In the early stage, our intention was to use our matching stage not only to identify the correct object ID but also to estimate the initial pose for further pose estimation in the second step. We aimed to achieve this by selecting matches with the highest similarity scores corresponding to the predicted object ID. However, as illustrated in Figure 5, we observed that this approach did not yield successful results, mostly due to DINOv2, but also the domain gap arising from differences in lighting conditions between the proposals and templates, and occlusions. It is worth noting that DINOv2 was trained using self-supervised learning with ro-

tation augmentation, there the model has some invariance to pose unfortunately. Although we treat this experiment as a negative result, we hope it provides valuable insights for the community.

5. Conclusion

We present a simple approach for novel object segmentation solely based on their CAD models, without the need for retraining. Surprisingly, our method achieves a remarkably high accuracy, comparable to previous supervised methods trained on extensive annotated data of testing objects. We hope that our approach will serve as a standard baseline for CAD-based novel object segmentation and will be employed as the initial stage for novel object pose estimation methods.

Acknowledgments. We thank Nermin Samet for helpful discussions. This research was produced within the framework of Energy4Climate Interdisciplinary Center (E4C) of IP Paris and Ecole des Ponts ParisTech, and was supported by 3rd *Programme d'Investissements d'Avenir* [ANR-18-EUR-0006-02] and by the Foundation of Ecole polytechnique (Chaire “Défis Technologiques pour une Énergie Responsable” financed by TotalEnergies). This work was performed using HPC resources from GENCI-IDRIS 2022-AD011012294R2.

References

- [1] Eric Brachmann, Alexander Krull, Frank Michel, Stefan Gumhold, Jamie Shotton, and Carsten Rother. Learning 6D Object Pose Estimation Using 3D Object Coordinates. In *European Conference on Computer Vision*, 2014. 4, 5, 6
- [2] Jianqiu Chen, Mingshan Sun, Tianpeng Bao, Rui Zhao, Liwei Wu, and Zhenyu He. 3d model-based zero-shot pose estimation pipeline. *arXiv preprint arXiv:2305.17934*, 2023. 1, 2, 4, 5
- [3] Maximilian Denninger, Martin Sundermeyer, Dominik Winkelbauer, Youssef Zidan, Dmitry Olefir, Mohamad Elbadrawy, Ahsan Lodhi, and Harinandan Katam. Blender-Proc. In *arXiv Preprint*, 2019. 1, 2, 5, 6
- [4] Andreas Doumanoglou, Rigas Kouskouridas, Sotiris Malasiotis, and Tae-Kyun Kim. Recovering 6d object pose and predicting next-best-view in the crowd. In *CVPR*, 2016. 4
- [5] Bertram Drost, Markus Ulrich, Paul Bergmann, Philipp Hartinger, and Carsten Steger. Introducing mvtec itodd-a dataset for 3d object recognition in industry. In *ICCV Workshops*, 2017. 4
- [6] Yuming Du, Wen Guo, Yang Xiao, and Vincent Lepetit. 1st Place Solution for the UVO Challenge on Image-based Open-World Segmentation 2021. In *ICCV Workshops*, 2021. 2
- [7] Yuming Du, Yang Xiao, and Vincent Lepetit. Learning to Better Segment Objects from Unseen Classes with Unlabeled Videos. In *International Conference on Computer Vision*, 2021. 2
- [8] Rohit Girdhar, Alaaeldin El-Nouby, Zhuang Liu, Mannat Singh, Kalyan Vasudev Alwala, Armand Joulin, and Ishan Misra. Imagebind: One embedding space to bind them all. In *Proceedings of the IEEE/CVF Conference on Computer Vision and Pattern Recognition*, pages 15180–15190, 2023. 2, 4
- [9] Kaiming He, Georgia Gkioxari, Piotr Dollár, and Ross Girshick. Mask r-cnn. In *Proceedings of the IEEE international conference on computer vision*, pages 2961–2969, 2017. 1, 2, 4, 5
- [10] Stefan Hinterstoisser, Vincent Lepetit, Slobodan Ilic, Stefan Holzer, Gary R. Bradski, Kurt Konolige, and Nassir Navab. Model Based Training, Detection and Pose Estimation of Texture-Less 3D Objects in Heavily Cluttered Scenes. In *Asian Conference on Computer Vision*, 2012. 3
- [11] Tomas Hodan, Pavel Haluza, Stepan Obdrzalek, Jiri Matas, Manolis Lourakis, and Xenophon Zabulis. T-LESS: An RGB-D Dataset for 6D Pose Estimation of Texture-Less Objects. In *IEEE Winter Conference on Applications of Computer Vision*, 2017. 4
- [12] Tomas Hodan, Frank Michel, Eric Brachmann, Wadim Kehl, Anders GlentBuch, Dirk Kraft, Bertram Drost, Joel Vidal, Stephan Ihrke, Xenophon Zabulis, et al. Bop: Benchmark for 6d object pose estimation. In *ECCV*, 2018. 4
- [13] Roman Kaskman, Sergey Zakharov, Ivan Shugurov, and Slobodan Ilic. Homebreweddb: Rgb-d dataset for 6d pose estimation of 3d objects. In *ICCV Workshops*, 2019. 4, 5, 6
- [14] Alexander Kirillov, Eric Mintun, Nikhila Ravi, Hanzi Mao, Chloe Rolland, Laura Gustafson, Tete Xiao, Spencer Whitehead, Alexander C Berg, Wan-Yen Lo, et al. Segment anything. *arXiv preprint arXiv:2304.02643*, 2023. 1, 2, 3, 4
- [15] Yann Labbé, Justin Carpentier, Mathieu Aubry, and Josef Sivic. CosyPose: Consistent Multi-View Multi-Object 6D Pose Estimation. In *European Conference on Computer Vision*, 2020. 1, 2, 4
- [16] Yann Labbé, Lucas Manuelli, Arsalan Mousavian, Stephen Tyree, Stan Birchfield, Jonathan Tremblay, Justin Carpentier, Mathieu Aubry, Dieter Fox, and Josef Sivic. MegaPose: 6D Pose Estimation of Novel Objects via Render & Compare. In *CoRL*, 2022. 1
- [17] Van Nguyen Nguyen, Yuming Du, Yang Xiao, Michael Ramamonjisoa, and Vincent Lepetit. PIZZA: A Powerful Image-only Zero-Shot Zero-CAD Approach to 6 DoF Tracking. In *International Conference on 3D Vision*, 2022. 2
- [18] Van Nguyen Nguyen, Yinlin Hu, Yang Xiao, Mathieu Salzmann, and Vincent Lepetit. Templates for 3D Object Pose Estimation Revisited: Generalization to New Objects and Robustness to Occlusions. In *Conference on Computer Vision and Pattern Recognition*, 2022. 1, 3
- [19] Maxime Oquab, Timothée Darcet, Théo Moutakanni, Huy Vo, Marc Szafraniec, Vasil Khalidov, Pierre Fernandez, Daniel Haziza, Francisco Massa, Alaaeldin El-Nouby, et al. Dinov2: Learning robust visual features without supervision. *arXiv preprint arXiv:2304.07193*, 2023. 1, 2, 4, 5
- [20] Pyrender. <https://github.com/mmatl/pyrender>. 3, 4, 5, 6
- [21] Yongzhi Su, Mahdi Saleh, Torben Fetzner, Jason Rambach, Nassir Navab, Benjamin Busam, Didier Stricker, and Federico Tombari. ZebraPose: Coarse to Fine Surface Encoding

- for 6 DoF Object Pose Estimation. In *Conference on Computer Vision and Pattern Recognition*, 2022. 1, 4, 5
- [22] Martin Sundermeyer, Tomáš Hodaň, Yann Labbe, Gu Wang, Eric Brachmann, Bertram Drost, Carsten Rother, and Jiří Matas. Bop challenge 2022 on detection, segmentation and pose estimation of specific rigid objects. In *Proceedings of the IEEE/CVF Conference on Computer Vision and Pattern Recognition*, pages 2784–2793, 2023. 1, 2, 4, 5
- [23] Gu Wang, Fabian Manhardt, Federico Tombari, and Xiangyang Ji. GDR-Net: Geometry-guided direct regression network for monocular 6d object pose estimation. In *IEEE/CVF Conference on Computer Vision and Pattern Recognition (CVPR)*, pages 16611–16621, June 2021. 1, 2
- [24] Yu Xiang, Tanner Schmidt, Venkatraman Narayanan, and Dieter Fox. PoseCNN: A convolutional neural network for 6D object pose estimation in cluttered scenes. In *RSS*, 2018. 4, 5, 6
- [25] Yu Xiang, Christopher Xie, Arsalan Mousavian, and Dieter Fox. Learning rgb-d feature embeddings for unseen object instance segmentation. In *Conference on Robot Learning*, pages 461–470. PMLR, 2021. 2
- [26] Christopher Xie, Yu Xiang, Arsalan Mousavian, and Dieter Fox. Unseen object instance segmentation for robotic environments. *IEEE Transactions on Robotics*, 37(5):1343–1359, 2021. 2
- [27] Xu Zhao, Wenchao Ding, Yongqi An, Yinglong Du, Tao Yu, Min Li, Ming Tang, and Jinqiao Wang. Fast segment anything. *arXiv preprint arXiv:2306.12156*, 2023. 1, 2, 3, 4